Mon. Not. R. Astron. Soc. **000**, 000–000 (0000) Printed 21 January 2014 (MN LATEX style file v2.2)

Tracing sunspot groups to determine angular momentum transfer on the Sun

D. Sudar[1] I. Skokić[2] D. Ruždjak[1] R. Brajša[1] H. Wöhl[3]
[1] *Hvar Observatory, Faculty of Geodesy, Kačićeva 26, University of Zagreb, 10000 Zagreb, Croatia*
[2] *Cybrotech Ltd, Bohinjska 11, 10000 Zagreb, Croatia*
[3] *Kiepenheuer-Institut für Sonnenphysik, Schöneckstr. 6, 79104 Freiburg, Germany*

Release 21 January 2014

ABSTRACT
The goal of this paper is to investigate Reynolds stresses and to check if it is plausible that they are responsible for angular momentum transfer toward the solar equator. We also analysed meridional velocity, rotation velocity residuals and correlation between the velocities. We used sunspot groups position measurements from GPR (Greenwich Photographic Result) and SOON/USAF/NOAA (Solar Observing Optical Network/United States Air Force/National Oceanic and Atmospheric Administration) databases covering the period from 1878 until 2011. In order to calculate velocities we used daily motion of sunspot groups. The sample was also limited to ±58°in Central Meridian Distance (CMD) in order to avoid solar limb effects. We mainly investigated velocity patterns depending on solar cycle phase and latitude. We found that meridional motion of sunspot groups is toward the centre of activity from all available latitudes and in all phases of the solar cycle. The range of meridional velocities is ±10 m s^{-1}. Horizontal Reynolds stress is negative at all available latitudes and indicates that there is a minimum value ($q \approx$ - 3000 m^2 s^{-2}) located at $b \approx \pm 30°$. In our convention this means that angular momentum is transported toward the solar equator in agreement with the observed rotational profile of the Sun.

Key words: Sun: rotation - sunspots - Sun: photosphere - Sun: activity

1 INTRODUCTION

Tracing the motion of sunspot groups has a long history and is still used frequently today for studies of solar rotation and related phenomena. In this work we used daily motion of sunspot groups from GPR (Greenwich Photographic Result) and SOON/USAF/NOAA (Solar Observing Optical Network/United States Air Force/National Oceanic and Atmospheric Administration) databases combined into a single dataset. The key parameter we will investigate is horizontal Reynolds stress which might explain the transfer of angular momentum toward the equator. In a review by Schröter (1985), the author advocated the use of sunspot data since both components of horizontal Reynolds stress can be measured separately. GPR dataset complemented by SOON/USAF/NOAA is the longest homogeneous sunspot catalogue and presents a unique opportunity to study long term average properties of the solar velocity field as well as its variations on time scale of a century. The GPR dataset we used was digitised in the frame of several projects and it is not identical to the on-line version[1]. Various analyses were carried out by using whole or parts of our GPR dataset (Balthasar & Wöhl 1980, 1981; Arévalo et al. 1982, 1983; Balthasar, Vázquez & Wöhl 1986; Balthasar, Wöhl & Stark 1987; Brajša & Wöhl 2000; Wöhl & Brajša 2001; Brajša et al. 2002, 2004; Ruždjak et al. 2004, 2005; Brajša et al. 2006, 2007).

A very comprehensive analysis of cycle to cycle variations of rotation velocity for GPR dataset is given in Balthasar et al. (1986) and Brajša et al. (2006). The same authors analysed also rotation velocity variations with respect to phase of the solar cycle.

Recently, a comprehensive project of revising the GPR dataset was undertaken (Willis et al. 2013a,b; Erwin et al. 2013) to correct a number of erroneous measurements and typos which illustrates the importance of the GPR dataset.

Various aspects of solar rotation and related phenomena are used to quantify and constrain solar models. Usually the main focus of such investigations are meridional motions and rotation residual velocity. Correlation between two velocities and their covariance are of even greater significance. All of these quantities play an important part in understanding the solar cycle and its variations from one cycle to another. Series of numerical simulations and theo-

[1] http://solarscience.msfc.nasa.gov/greenwch.shtml

retical works regarding the transfer of angular momentum toward the equator has been carried out by many authors (Canuto, Minotti & Schilling 1994; Chan 2001; Rüdiger & Hollerbach 2004; Käpylä, Korpi & Tuominen 2004; Hupfer, Käpylä & Stix 2006).

Studies of meridional flows show wide discrepancy in their results both qualitatively and quantitatively. By analysing sunspot groups data obtained at Mount Wilson Howard & Gilman (1986) found that for lower solar latitudes ($b < \pm 15^\circ$) meridional motion is negative, i.e. toward the equator. The magnitude of the effect being $\omega_{mer} \approx 0.02^\circ \mathrm{day}^{-1}$. Above mentioned latitude, the flow is toward the poles with a possible hint that at even higher latitudes it changes sign again. Wöhl & Brajša (2001) studied meridional motion of stable recurrent sunspot groups and they also found that the average flow is equatorward for lower latitudes, while poleward motion occurs at latitudes higher than latitude of the centre of activity. Moreover, the magnitude of the effect is the same as that of Howard & Gilman (1986). But their data does not provide any indication that the flow might change to equatorward at even higher latitudes. By studying sunspot drawings obtained at National Astronomical Observatory of Japan during the years 1954-1986, Kambry et al. (1991) found that meridional flow is equatorward for latitudes in the range -20° to +15°. They also found an indication of a solar-cycle dependence of meridional motions. Howard (1991b, 1996) found that sunspot groups move away from the average latitude of activity while plages move toward it.

By using Doppler line shifts, Duvall (1979) observed roughly constant poleward flow on the order of v_{mer} =20 m s^{-1} in the whole range of studied latitudes (10° - 50°). Howard (1979) mentions the same value, but referring only to *higher latitudes*. By analysing Doppler velocity data obtained with the Global Oscillating Network Group (GONG) instruments, Hathaway (1996) concluded that the flow is poleward at all latitudes with typical values being about v_{mer} =20 m s^{-1}, but with episodes of much stronger flows (60 m s^{-1}). In contrast to the above, Pérez Garde et al. (1981) found equatorward motion of $v_{mer} \approx 20$ m s^{-1}. Lustig & Wöhl (1990) studied meridional plasma motions using Doppler line shifts covering the period from 1982 until 1986, covering about a half of the solar cycle. The authors concluded that systematic meridional motion, if even present at all, can not be larger than v_{mer} =10 m s^{-1} toward solar equator for latitudes below $b = \pm 35^\circ$ in both hemispheres.

Using high-resolution magnetograms taken from 1978 to 1990 with the NSO Vacuum Telescope on Kitt Peak, Komm et al. (1993) observed poleward flow of the order of v_{mer} =10 m s^{-1} in both hemispheres. The flow increased in amplitude from 0 m s^{-1} at the equator, reached a maximum at mid-latitude and slowly decreased at even higher latitudes. By applying time-distance helioseismology, Zhao & Kosovichev (2004) found poleward meridional flows of the order of v_{mer} =20 m s^{-1}. In addition they found meridional circulation cells converging toward the activity belts in both hemispheres.

Apart from evolutionary loss of angular momentum (see, e.g., Guinan & Engle 2009), the Sun also exhibits changes of the rotational profile on much smaller time scales. A cyclic pattern with a period of ≈11 years of alternating faster and slower rotational bands is called torsional oscillations. Existence of torsional oscillations on the Sun were first reported by Howard & Labonte (1980). They were further confirmed by Ulrich et al. (1988), Howe et al. (2000), Haber et al. (2002), Basu & Antia (2003) and others. At latitudes below $b \approx \pm 40^\circ$ bands propagate equatorward while each band is about 15° wide in latitude. The amplitude of the effect is about Δv_{rot} =5-10 m s^{-1}. Brajša et al. (2006) showed an interesting analysis of rotation velocity residuals versus phase of the solar cycle in their Fig. 6 showing variations of $\Delta\omega_{rot} \approx 0.05$ ° day^{-1} corresponding to $\Delta v_{rot} \approx 7$ m s^{-1} at the equator.

Transfer of the angular momentum from higher to lower latitudes can be revealed by studying the correlation and covariance between azimuthal and meridional flows. Covariance, denoted as $Q =< \Delta v_{rot} v_{mer} >$, is a horizontal Reynolds stress. Reynolds stress is thought to be the main generator of maintaining current differential rotation profile (see, e.g., Pulkkinen & Tuominen 1998; Rüdiger & Hollerbach 2004). Indeed, observations seems to show that the correct value of Q was observed (Ward 1965; Belvedere et al. 1976; Schröter & Wöhl 1976; Gilman & Howard 1984; Pulkkinen & Tuominen 1998; Vršnak et al. 2003). In addition, some authors (Ward 1965; Gilman & Howard 1984; Pulkkinen & Tuominen 1998; Vršnak et al. 2003) investigated latitudinal dependence of Reynolds stress, and found that it mainly decreases with higher latitudes with a possible minimum around $b = \pm 30^\circ$.

2 DATA AND REDUCTION METHODS

We limited the data to ±58° in Central Meridian Distance (CMD) which corresponds to about 0.85 of projected solar radius (cf. Balthasar et al. 1986). With such cutoff we obtained a sample of 92091 data pairs from GPR to obtain rotation rates and meridional velocities. We used two subsequent measurements of individual sunspot group to get one velocity value.

Using the same CMD cutoff, we ended up with a sample of 43583 data pairs from observations found in SOON/USAF/NOAA database in the period from 1977 until 2011. Combining these samples into a single dataset the total amount of data points for sunspot groups was 135674 spanning from year 1878 till 2011. In the rest of this work we will refer to this combined dataset as EGR (Extended Greenwich Result). In the GPR era (until 1977), positions of sunspot groups are given with accuracy of 0.1° in both coordinates while subsequent measurements were usually taken 1 day apart. After 1977 the positions are usually given with the accuracy of 1.0°.

When observed by tracers, solar rotation and related phenomena should be treated statistically which requires large number of measurements for proper analysis. While solar rotation velocity has large signal to noise ratio, (S/N), solar rotation residuals, meridional velocities and Reynolds stress are significantly weaker effects with lower S/N. So, in this paper we will mostly concentrate to identify basic net effect in various relationships between mentioned phenomena.

Meridional motion and angular rotation velocity were calculated from two subsequent measurements of position. Since most of the measurements in our dataset are one day

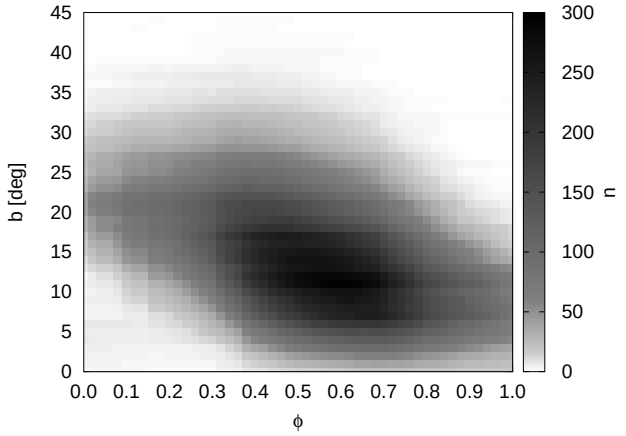

Figure 1. Latitudinal distribution of sunspot groups from EGR dataset with respect to phase of the solar cycle, ϕ. All data are folded into one solar hemisphere.

apart, velocities are calculated from daily shifts of sunspot groups. To obtain rotation velocity residuals it is necessary to subtract the actual velocity measured from the average rotation velocity at given latitude. Synodic angular velocities were calculated by using the daily motion of sunspot groups and converted to sidereal angular velocities using the procedure described in Roša et al. (1995) and Brajša et al. (2002). Due to latitudinal distribution of sunspots it is sufficient to use only the first two terms in the standard solar differential rotation equation:

$$\omega(b) = A + B \sin^2 b, \tag{1}$$

where b is the heliographic latitude and $\omega(b)$ is sidereal angular velocity.

For the EGR dataset we obtained $A = 14.499 \pm 0.005^\circ$ per day and $B = -2.64 \pm 0.05^\circ$ per day that we calculated by fitting the above equation to all points in the dataset ($n = 135674$).

After the subtraction was carried out angular velocity residuals have been transformed to linear velocities residuals (Δv_{rot}) in meters per second, taking into account latitudes of the tracers. Solar radius used for conversion from angular velocities to linear velocities was $R_\odot = 696.26 \cdot 10^3$ km (Stix 1989).

We limited calculated sidereal rotation velocity to 8 - 19° per day in order to eliminate any gross errors usually resulting from misidentification of sunspot groups or typos.

Angular meridional velocities were also transformed to linear velocities in m s^{-1}.

In the following section we will present several map plots of various quantities depending on latitude, b, and phase of the solar cycle, ϕ. Therefore, it is useful to show latitudinal distribution of sunspots from EGR dataset with respect to phase of the solar cycle, ϕ, in order to indicate where the results are more reliable (Fig. 1). We folded all the data into one solar hemisphere.

In order to determine the phase we used times of minima and maxima of solar activity found in Table 1 from Brajša et al. (2009). All points that belong after the minimum of the solar cycle and before maximum were mapped to $[0, 0.5]$ phase range. Points after the maximum, but before the minimum of the next cycle, were assigned phase in $[0.5, 1]$ range. Phase was calculated in a linear scale:

$$\phi_i = \frac{t_i - t_{min/max}}{t_{max/min} - t_{min/max}}. \tag{2}$$

Since distribution of sunspots in latitude is not uniform, some precaution must be used in order not to detect false motion (Olemskoy & Kitchatinov 2005). Calculated velocities need to be assigned to some latitude. Considering we have two measurements of position for one velocity, we have to decide to which latitude we should assign the velocity. Olemskoy & Kitchatinov (2005) showed that false flow can arise if average latitude of the two values is used, since the gradient of sunspot latitudinal distribution will pollute the result. They also showed that this false meridional flow is of the right order of magnitude and in the right direction as the results obtained by many authors using tracers to detect surface flows on the sun. However, there is a simple solution to this problem: if we assign the velocity to the latitude of the first measurement of position, there is no net flow into the latitude bin from other latitudes and we don't have to worry about the non-uniform distribution of sunspots in latitude. Olemskoy & Kitchatinov (2005) also concluded the same.

3 RESULTS

3.1 Meridional flow

We used the convention that negative meridional velocity reflects equatorward motion: $v_{mer} = -\partial b/\partial t$ for southern hemisphere, where we have defined southern latitudes as negative values.

In this section we investigate the properties of v_{mer} depending on latitude, b, and phase of the solar cycle, ϕ. In Fig. 2 we show a map plot of v_{mer} versus cycle phase and latitude, b, for EGR dataset. All points were folded into one phase diagram and both solar hemispheres were folded together according to our convention above. The map plot is constructed first by binning the data into square bins of width 0.1 in phase of the cycle, ϕ and height 1°in latitude. Then we calculated the average values of velocity in each bin, discarding all the bins where the number of data points was less than 10 (see Fig. 1). Finally we calculated smoothed averages of each bin with weight given by $w(d) = 1/(1+d^2)$, where d is a distance of each data point from the map grid point. Brighter shades of grey depict polewards motion ($v_{mer} > 0$), while darker shades show motion toward the solar equator ($v_{mer} < 0$). On the same plot we show a contour line of $v_{mer} = 0$ with a solid line which clearly separates the two regions of opposite meridional flow.

Such distinct appearance can be easily confirmed by plotting average values of v_{mer} in bins 2° wide in latitude (Fig. 3). This is similar to Fig. 2 only integrated in phase of the solar cycle, ϕ, or in other words integrated in time. In the same Fig. we show a linear fit of $v_{mer}(b)$ through individual data points, given by equation:

$$v_{mer} = (-0.571 \pm 0.038) \text{ m s}^{-1}(^\circ)^{-1} \cdot b + (8.61 \pm 0.64) \text{ m s}^{-1}. \tag{3}$$

From the above equation we get the intersect with x-axis, $v_{mer}(b) = 0$, for $b \approx 15^\circ$. In the inset to Fig. 3 we show average values of v_{mer} separately for the two solar hemispheres.

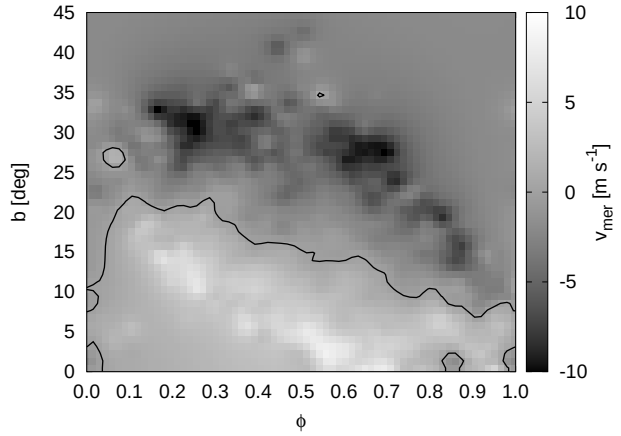

Figure 2. Map plot of meridional velocity, v_{mer}, versus phase of the solar cycle, ϕ, and latitude, b. Also shown is a contour line where $v_{mer} = 0$ with a solid line.

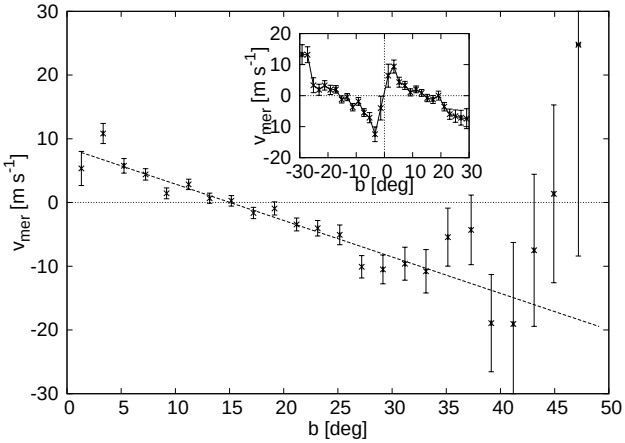

Figure 3. Average values of v_{mer} in bins 2° wide in latitude, b. Linear fit (Eq. 3) is shown with a dashed line. In the inset we show average values v_{mer} for North and South solar hemisphere separated.

We can see that for very low latitudes v_{mer} goes back to zero and reverses sign when crossing the solar equator.

We also divided the data into 10 bins in phase, ϕ, each being 0.1 wide. Then we calculated $v_{mer}(b)$ linear fits for those 10 bins. The coefficients, given by equation:

$$v_{mer} = c_1 b + c_2, \tag{4}$$

are shown in Table 1.

Perhaps the most interesting result is that the contour line from Fig. 2 representing values $v_{mer} = 0$ is very close to centre of activity in each phase, i.e. average latitude as a function of phase, $\overline{b(\phi)}$. Average latitude, $\overline{b(\phi)}$, was calculated with $\overline{b(\phi)} = \sum b_i/n(\phi)$ (sunspot group area was not taken into account). Therefore, we calculated values of b_0, for which $v_{mer} = 0$, in all 10 phase bins ($b_0 = -c_2/c_1$). The values are given in Table 1 next to $\overline{b(\phi)}$. Both quantities are shown in Fig. 4. Average latitudes, $\overline{b(\phi)}$, are drawn with a dashed line and solid circles, while b_0 is drawn with a thin solid line, solid triangles and error bars. The error bar for phase ϕ=0.05 is off the scale. We also showed the contour line for $v_{mer} = 0$ obtained from the map plot presented in Fig. 2. Apart from the highly uncertain value of b_0 for phase $\phi < 0.1$ the agreement between b_0 and $\overline{b(\phi)}$ is very good.

Table 1. Values of linear fit coefficients (Eq. 4), intersect with x-axis, $b_{v_{mer}=0}$, and average latitude of sunspot groups, $\overline{b(\phi)}$.

ϕ	c_1[m s^{-1} (°)$^{-1}$]	c_2[m s^{-1}]	$b_{v_{mer}=0}$[°]	$\overline{b(\phi)}$[°]
0.05	-0.11±0.22	0.3±4.8	2.7±43.8	19.3
0.15	-0.51±0.23	10.3±5.5	19.9±13.9	22.0
0.25	-0.94±0.17	20.5±3.7	21.8±5.5	21.1
0.35	-0.83±0.12	15.4±2.5	18.6±4.0	19.1
0.45	-0.65±0.11	10.6±1.9	16.3±4.0	16.9
0.55	-0.63±0.09	10.2±1.3	16.1±2.9	15.0
0.65	-0.73±0.10	9.6±1.4	13.2±2.6	13.1
0.75	-0.88±0.15	9.2±1.8	10.4±2.7	11.4
0.85	-1.20±0.24	11.1±2.7	9.3±2.9	9.9
0.95	-0.73±0.30	5.8±3.4	8.0±5.6	9.5

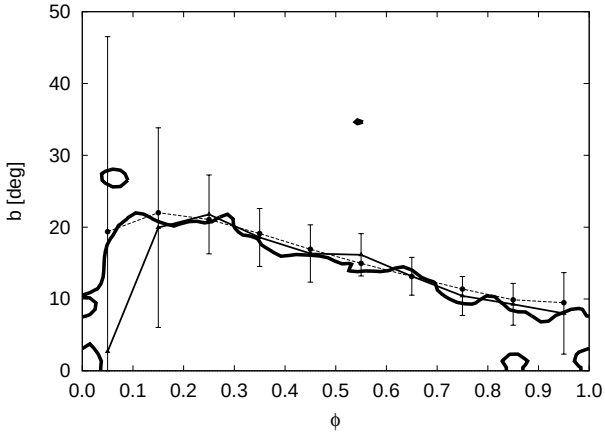

Figure 4. Values of $b_0 = c_2/c_1$ for 10 phase bins with error bars (solid line with solid triangles), $\overline{b(\phi)}$ (dashed line with solid circles) and contour line of $v_{mer} = 0$ (thick solid line).

Regions with latitudes closer to solar equator move toward the pole, while centre of activity in each phase roughly marks the line where meridional motion changes to equatorward motion.

3.2 Torsional oscillations

Torsional oscillations can be described as a pattern in which the solar rotation is sped up or slowed down in certain regions of latitude. In this section we will investigate if we can reveal this pattern by examining the Δv_{rot} relationship with latitude, b, and cycle phase, ϕ.

We constructed a map plot of Δv_{rot} (Fig. 5) in the same fashion as in the previous section. Thick dashed lines show a contour where $\Delta v_{rot} = 0$, darker regions depict slower than average rotation ($\Delta v_{rot} < 0$), while brighter regions show faster then average rotation ($\Delta v_{rot} > 0$). Fig. 5 shows a rather complex pattern of rotation velocity residuals. The pattern does not look like a typical torsional oscillation pattern. In order to investigate if the typical torsional oscillation pattern is only present in today's data, we divided our

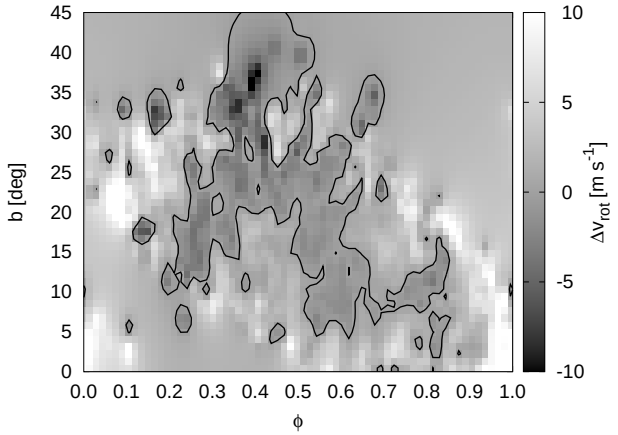

Figure 5. Map plot of Δv_{rot} as a function of phase of the solar cycle, ϕ, and latitude b.

dataset into three epochs: early (cycles 12 - 15), mid (cycles 16 - 19) and late (cycles 20 - 24) and plotted the same type of plot (Fig. 6). However, the figure doesn't reveal anything that even resembles the typical torsional oscillation pattern. Moreover, results from three different epochs are not consistent between themselves and we can't see any regularity in changes of the pattern over time. With our dataset it is not possible to make the division into shorter epochs, because as we can see from the top part of Fig. 6 we are already running out of datapoints at latitudes above 30°.

3.3 Correlation of v_{mer} and Δv_{rot} and covariance $< v_{mer}\Delta v_{rot} >$

In this section we will investigate correlation and covariance of meridional velocity, v_{mer}, and rotation velocity residuals, Δv_{rot}. Due to our convention that negative meridional motion reflects equatorward motion, it follows that negative values of covariance, q, means that angular momentum is also transported toward the solar equator.

In Fig. 7 we show $v_{mer}(\Delta v_{rot})$ relationship. The least squares linear fit is described by the following relation:

$$v_{mer} = (-0.0804 \pm 0.0017) \cdot \Delta v_{rot} + (-0.12 \pm 0.27) \text{ m s}^{-1} \quad (5)$$

and is shown on the figure with the solid line.

Howard (1984) criticised usage of sunspot groups to derive correlation between v_{mer} and Δv_{rot}. Because of the average sunspot group tilt of about 4° (Howard 1991a) toward the equator one can imagine that as the group evolves, measured position of the group could be biased toward the tilt line. Consequently, derived velocities would also be biased and would produce just the type of correlation between v_{mer} and Δv_{rot} as we see in Fig. 7 and Eq. 5. However, it is very difficult to actually quantify the magnitude of this effect and to conclude how much it would influence the true correlation between the two velocities. By using coronal bright points (CBP) as tracers, Vršnak et al. (2003) derived almost the same correlation. The tilt angle is irrelevant for CBPs and this is our first hint from independent measurements that the bias mentioned by Howard (1984) is negligible or not present at all. GPR catalogue also contains the information about the morphological type of the sunspot group. Quite

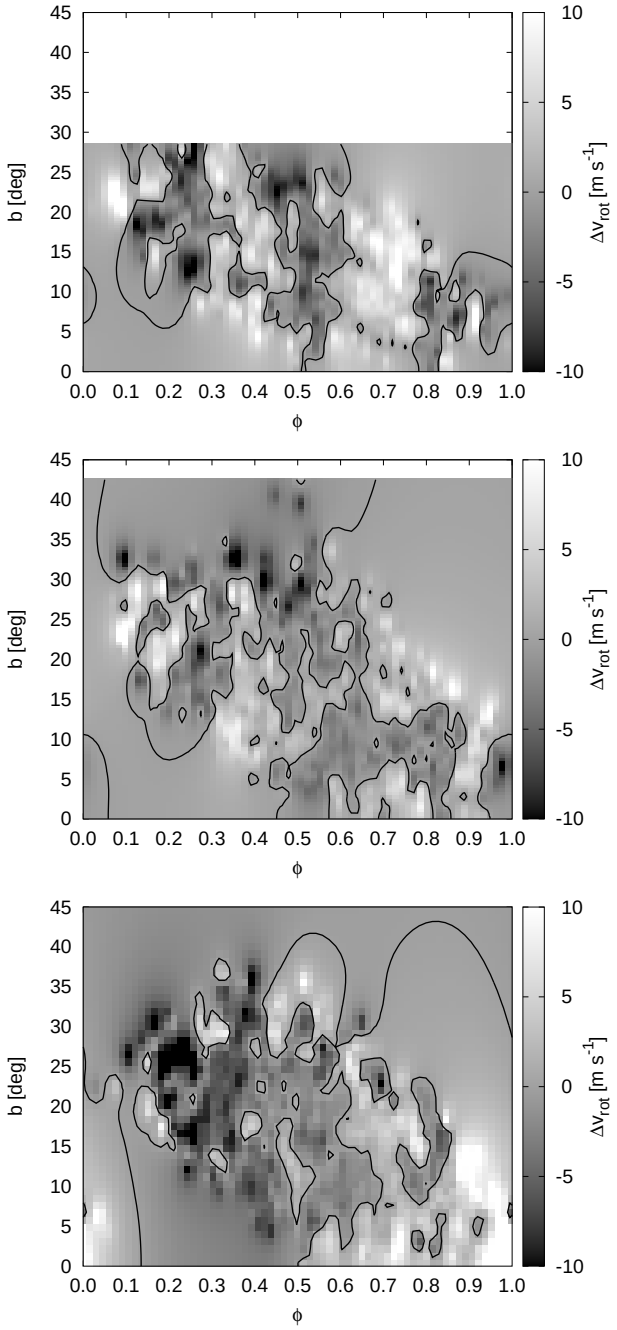

Figure 6. The same as in Fig. 5 except that the EGR dataset is divided into three epochs. From top to bottom we show early epoch (cycles 12 - 15), mid (cycles 16 - 19) and late (20 - 24). In early epoch (top figure) there is insufficient number of data points for latitudes above ≈30°.

a significant number of them are actually classified as a single spot. Tilt angle for such groups is meaningless and no such bias can exist for this subset. Therefore, we checked the correlation between v_{mer} and Δv_{rot} for this subset of single spots and obtained:

$$v_{mer} = (-0.0803 \pm 0.0036) \cdot \Delta v_{rot} + (-1.40 \pm 0.46) \text{ m s}^{-1}. \quad (6)$$

The correlation is virtually identical to the one obtained for all groups (Eq. 5). This is a conclusive proof that the group

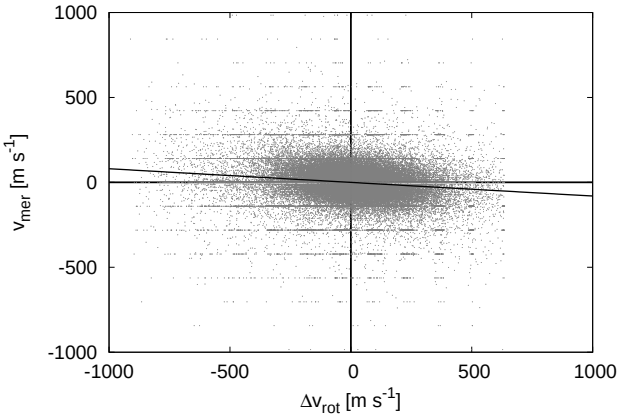

Figure 7. Correlation between meridional velocity, v_{mer}, and rotation velocity residual, Δv_{rot}, for sunspot groups. Linear fit is shown with a solid line.

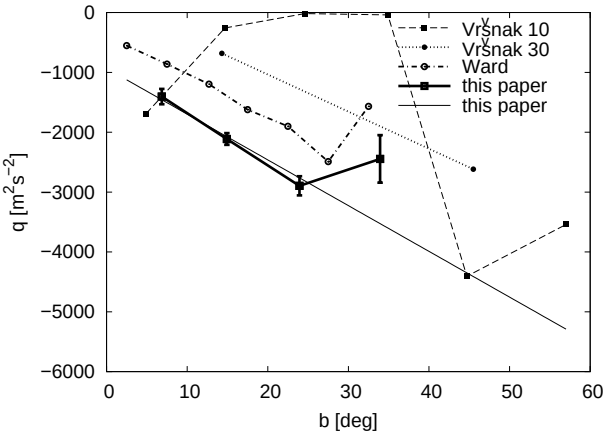

Figure 8. Relationship between covariance, q, and latitude, b, represented by average values in bins of different width obtained with data from this paper and other authors. Results from Ward (1965) are labelled Ward and results from Vršnak et al. (2003) are labelled Vršnak 10 and Vršnak 30 for their bins of 10 and 30 degrees, respectively. Linear fit (Eq. 7) is shown with a thin solid line.

Table 2. Average value of covariance, q, for several bins in latitude, b.

bin	q[m^2 s^{-2}]	b[°]	n
$0° < b < 10°$	-1404±128	6.85	35836
$10° < b < 20°$	-2113±98	14.93	67156
$20° < b < 30°$	-2896±160	23.93	28518
$b > 30°$	-2446±397	33.953	4164

tilt bias is not significantly affecting the observed correlation when using sunspot groups as tracers. In Fig. 7 there are visible artefacts in the form of horizontal lines which correspond to steps of 1 deg/day. They are a consequence of poor precision of position in SOON/USAF/NOAA part of the dataset which is usually recorded with 1 deg precision only. Coupled with usual 1 day period between successive measurements we get the horizontal artefacts separated by 1 deg/day. However, we note that they do not significantly affect the results, since whole SOON/USAF/NOAA part of the dataset was excluded from calculations given in Eq. 6 because this part of the dataset does not contain the information on the morphological type of the sunspot groups.

We also investigated if averages of $< \Delta v_{rot} v_{mer} >$ grouped in bins of 10° will show any dependence of q with latitude. We grouped the dataset into four subsets spanning from 0° to 10°, 10° to 20°, 20° to 30° and above 30° in latitude and then simply calculated the averages of $\Delta v_{rot} v_{mer}$ product for each bin to obtain $q(b)$ values. The results are given in Table 2 and shown on Fig. 8. On the same figure we also show results obtained by Vršnak et al. (2003) (their 10° and 30° bins) and Ward (1965) and also a linear fit

$$q = (-76.4 \pm 9.5)\ \mathrm{m^2\ s^{-2}}(^\circ)^{-1} \cdot b + (-933 \pm 161)\ \mathrm{m^2\ s^{-2}} \quad (7)$$

through individual data points of our EGR dataset.

Finally, in Fig. 9 we show a map plot of covariance, q, as a function of phase of the solar cycle, ϕ, and latitude, b. In the same figure we outlined levels of $q = -2000$ m^2 s^{-2}, $q = -2500$ m^2 s^{-2} and $q = -2900$ m^2 s^{-2} with thinest to thickest solid line, respectively. This representation of covariance, q, is fairly consistent across all phases and latitudes with larger values of q concentrated around lower latitudes for all phases.

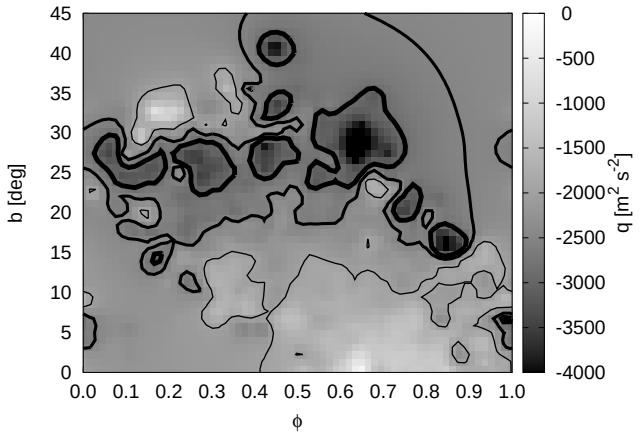

Figure 9. Map plot of covariance, q, versus phase of the solar cycle, ϕ, and latitude, b. Levels of $q = -2000$ m^2 s^{-1}, $q = -2500$ m^2 s^{-2} and $q = -2900$ m^2 s^{-2} are shown with solid lines, from thinest to thickest, respectively.

4 DISCUSSION

Before we comment on the results presented, we must clarify statistical significance of various types of plots shown in this work. Map plots have the lowest statistical significance because they show dependence of the variable with respect to two parameters which means that in each bin there are significantly fewer data points than in other plots. In this work these plots were used only as informative and not a single value was calculated from them. They do, however give a useful first look at data and various relationships.

Second type of plots show some empirical curve fitted

to the data with one variable and one parameter. These have higher importance because density of data points is significantly larger in one-dimensional parameter space than in two-dimensional. Nevertheless, caution must be taken before interpretation. Since fitted curves are only empirical, the form of the equation largely depends on how the raw data look like, rather then what it should be like from theoretical modelling. Typical example is shown in Fig. 3 where the linear function is fitted to the data. The look of the function might lead someone to believe that there is a positive meridional flow at 0 deg latitude. However, if we look at average values in bins of latitude (even more conclusively shown in the inset to Fig. 3), we see that the flow actually drops to zero for very low latitudes on both hemispheres. Values of parameters of the fitted linear function are dominated by mid-latitude behaviour where most of the data points actually are.

The third type of plots are plots where we show average values grouped in bins. Together with their errors, they should be the most reliable representation of what true relationship actually looks like.

4.1 Meridional motions

We have seen that meridional motions of sunspot groups show a distinct pattern where at latitudes below the centre of activity, the motion is poleward, while on the other side the motion is predominantly toward the equator. In addition we have shown that this is valid for all phases of the solar cycle. Flow converging to activity belts from both sides suggests that the plasma is circulating towards the centre of the Sun at these latitudes (sinking). Diverging flow on the equator suggest that the plasma is circulating from below to the surface. There might be another latitude point of diverging flow at about 40°, but our results are inconclusive if this diverging flow is real.

This result is in contradiction with most of the other results generated from tracer measurements (Howard 1991b, 1996; Snodgrass & Dailey 1996; Vršnak et al. 2003). In most of them the flow is opposite to ours; they found meridional flow to be out from the centre of activity. Although, none of the above papers mention to which latitude calculated velocity is assigned to, we suggest that their result is a consequence of not properly accounting for non-uniform latitudinal distribution of tracers they used. Moreover, if we use any of the other two possibilities (average latitude or latitude of the second measurement of position) we get almost exactly the opposite flow. Our approach, used in this paper, eliminates the need to keep track of tracer distribution and shows the true meridional motion.

Helioseismology measurements usually detect predominant poleward flow at all latitudes (Zhao & Kosovichev 2004; González Hernández et al. 2008, 2010). However, there is a striking similarity between our results for meridional flow (Figs. 2 and 3) and *residual* meridional flow found by helioseismology (Zhao & Kosovichev 2004; González Hernández et al. 2008, 2010). For example all details from our Fig. 3 are reproduced in González Hernández et al. (2008). This includes the change from equatorward to poleward flow at about 40°of latitude, even though our results are highly uncertain at these high latitudes. Zhao & Kosovichev (2004) explicitly state that residual meridional flow is converging toward activity belts. This raises the question, why we can't see the dominant poleward flow in tracer measurements? One possibility is that this flow is not constant in time and that it was different in the past which averages to net zero flow and we only observe residual which is permanent.

Hathaway (2012) used supergranules as probes of the Sun's meridional circulation. He found that surface poleward flow gradually changes to equatorward as we go deeper below solar surface. One of the intermediate between those two extremes might be the results we obtained by tracing sunspot groups. Ruždjak et al. (2004) suggested that at their birth sunspots groups could be coupled to the layer at about $r = 0.93\ R_\odot$ effectively showing the plasma flow from beneath the solar surface.

Another possibility to explain the difference between helioseismology and tracer measurements is that the flow is different around sunspots than in the rest of solar surface. With tracers we are confined to a small region of the solar disk around active regions, while helioseismology does not have this limitation.

4.2 Torsional oscillations

Torsional oscillation pattern is usually described as distinct bands of faster and slower than average rotation rate. These bands move toward the equator with time at low latitudes (see for example Basu & Antia 2003).

Our analysis of rotation velocity residuals reveals a pattern much less distinctive than for the meridional flow. Apart from generally remarking that slower than average flow is obtained around the maximum and faster than average around the minimum there is hardly anything else we could say about it. Similar behaviour was found by Brajša et al. (2006) and Brajša et al. (2007). It has no distinct latitudinal dependence and it shows no significant correlation with zones of activity. Zhao & Kosovichev (2004) showed zonal flows for years 1996-2002 (solar cycle 23) and it looks as if their results are similar to ours (faster than average in the phases around the minimum of solar activity and slower than average around the maximum). However, we can't confirm that the typical torsional oscillation pattern is visible in sunspot data.

We investigated the rotation residual flow in three different epochs to see if the typical torsional oscillation pattern can only be seen in modern data. The pattern does change with time, but it has no resemblance to torsional oscillations. Moreover, we can't see any regularity in it's shape and change from epoch to epoch. Thus we were unable to quantify dependence of rotation residuals with respect to phase and latitude. It's quite possible that we see only random noise.

4.3 Reynolds stress

From our Fig. 8, Eq. 7 and Table 2 it is easily seen that the equatorward angular momentum transfer is predominant at all latitudes covered by sunspot group data ($q < 0$). This is consistent with other studies using different methods and/or different data samples (Ward 1965; Gilman & Howard 1984; Vršnak et al. 2003).

Average values of q in 10° bins of b, shown in Table 2,

shows very similar behaviour to the linear fit for sunspot groups sample. Vršnak et al. (2003) showed similar results for 10° bins using CBP sample (their Fig. 6c), but the qualitative behaviour is different than ours. We suggest that this is due to their 10° bins being of too low statistical significance. This is also implied by their 30° bins which show different qualitative behaviour much more similar to ours. Moreover, our results for 10° bins show very similar behaviour to that of Ward (1965), both qualitatively and quantitatively.

Another interesting feature visible in Fig. 8 is that there appears to be a minimum in $q(b)$ relationship around 25-30°, both for our sample and for that given by Ward (1965). This is also reminiscent of similar result obtained by, for example, numerical simulations (Pulkkinen et al. 1993) and results obtained by Canuto et al. (1994) based on theoretical considerations. In order to investigate this a little more we plotted average values of covariance, q, with respect to latitude for both solar hemispheres separately (Fig. 10). In this representation negative values represent angular momentum transfer toward equator for northern solar hemisphere. On the southern hemisphere *positive* values of q also show momentum transfer toward the equator. So, this Fig. is consistent with Figs. 8 and 9 where we see equatorward momentum transfer at all available latitudes.

Since the minimum at around b =25-30°of latitude appears at all our plots we constructed an empirical relationship between q and b which takes into account dominant linear dependence for low latitudes and allows for a possible minimum at some unspecified latitude:

$$q = (e_1 b + e_2) \cdot e^{-e_3 b^2}. \quad (8)$$

This shape can produce a minimum, but could also 'explode' to $q = \pm\infty$, if e_3 turns out to be negative. By fitting through individual data points we obtained the coefficients of the fit shown in Table 3 and we also show the fit in Fig. 10 as a solid line.

The shape of the curve is very similar to that given by Canuto et al. (1994) in their Fig. 15 including the prediction that $q(b)$ falls to zero at the poles. The form of our fit function (Eq. 8) does not guarantee that, because the answer to the question if and where (in terms of b) covariance, q, falls to zero is highly sensitive to fitted coefficients and not constrained by the physical fact that maximum latitude is b =90°.

However, we must stress that although the agreement with Canuto et al. (1994) is good and that calculated coefficients seem strongly constrained (Table 3), latitudinal extent of sunspot groups is very limited and anything that happens beyond b =35-40°is ambiguous considering our dataset. Even the location and depth of the minimum is not very reliable for the same reason. Therefore, it is of great importance to confirm or disprove our hypothesis about the shape of $q(b)$ at mid to high latitudes.

The depth of the minimum, is also close to the one found by Canuto et al. (1994) considering that $q \approx -3000$ m^2 s^{-2} ≈ -0.15(°day^{-1})^2.

5 SUMMARY AND CONCLUSION

The most important results can be summarised as follows:

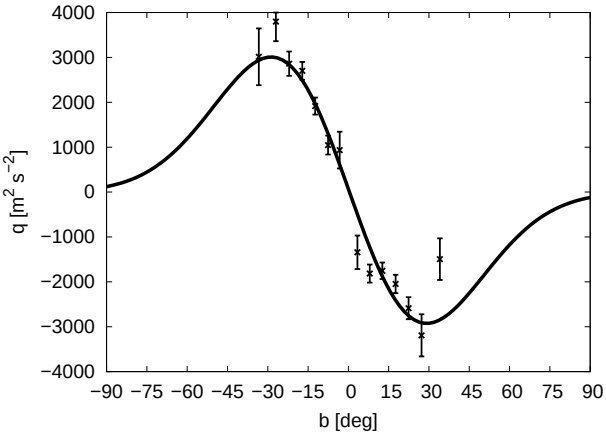

Figure 10. $q(b)$ relationship for EGR sample fitted with exponential cutoff model (solid line) and average values of q in bins spanning both solar hemispheres.

Table 3. Non linear fits coefficients for exponential cutoff model.

coefficient	value
e_1 [m (°)$^{-1}$ s^{-2}]	-169.0 ± 9.7
e_2 [m^2 s^{-2}]	69 ± 80
e_3 [(°)$^{-2}$]	0.00060 ± 0.00012

- Meridional motion of sunspot groups clearly shows poleward motion for all latitudes bellow the centre of activity and motion toward the equator for higher latitudes. This is valid for all phases of the solar cycle with a very strong correlation.
- The variations of v_{mer} with latitude, b, are approximately in the range of $v_{mer} = \pm 10$ m s^{-1}.
- Rotation velocity residuals show unusual torsional oscillation pattern. The actual values of rotation residual velocity rarely exceed Δv_{rot} =5 m s^{-1}. Rotation velocity residuals map plots in different epochs show a changing pattern which we are unable to explain. It is possible that we see only a pattern resulting from random errors.
- Meridional velocities are similar to *residual* meridional velocities found with time-distance helioseismology (Zhao & Kosovichev 2004; González Hernández et al. 2010).
- Reynolds stress is negative at all available latitudes which, in our convention, corresponds to equatorward transport of angular momentum. This supports the idea that observed rotational profile is actually driven by the Reynolds stress.
- Latitudinal dependence of Reynolds stress suggests a minimum at about $b \approx 30°$. The value of covariance being $q \approx$-0.15 (°)^2 day^{-2} ($q \approx$ - 3000 m^2 s^{-2}). This is consistent with Canuto et al. (1994).
- Phase and latitudinal dependence of covariance, q, seems to be fairly uniform in all phases of the solar cycle with possible exception at phases very late in the solar cycle.

Most authors who used tracers to track the meridional flow found meridional velocities to be opposite to ours. We believe that this is a consequence of improper assignment

of latitude to measured velocities. In the approach we used (assigning velocities to the starting latitude), latitudinal distribution of tracers is irrelevant because calculation of averages (and even fit functions) does not need to take into account the number of tracers at specific latitude ($n(b)$ is the same for all of them for each particular b). If we were to use average latitude between two successive measurement of position, we would have to calculate *weighted* averages by taking into account from which latitude the tracer actually started and assign weight accordingly.

As a test, we have also made an analysis with assigning the second latitude of two successive measurements and calculated average meridional motions and got the results very similar to, for example, Snodgrass & Dailey (1996) and Vršnak et al. (2003). Assigning second latitude or average latitude suffers from exactly the same problem; we would need to take into account the first latitude in order to properly calculate weighted averages. By using the starting latitude as the relevant one, we simply defined the flow as flow *from* certain latitude instead of flow *into* some latitude. There is no loss of generality in doing so and no difference in physical interpretation. Similar result for meridional velocity to ours was obtained by Olemskoy & Kitchatinov (2005) who pointed out the solution to this problem and used starting latitudes of the tracers. As a point of interest, even when we used the second latitude in our test, calculated correlation and covariance of meridional and residual rotation velocities was very similar to the results we obtained in this paper by using the first latitude. This also explains why our results, regarding correlation and covariance, are similar to the results of other authors who used tracers even if they found different average meridional flow than we did.

We can see a clear increase of uncertainties at latitudes larger than 30° which is a consequence of sunspot latitudinal distribution. Therefore, it is of great importance to use other methods or tracers (for example CBPs) to extend the analysis to higher latitudes.

The absence in our data of predominant poleward meridional flow which is found in helioseismology might be explained by several possibilities. The first one is that sunspots are anchored at depth below the surface showing sub-photospehric flow. Another possibility is that on longer time-scales the flow changes from poleward to equatorward and consequently averages out in our analysis. And finally, it is possible that the flow in active regions is different than in the rest of the solar disk, so in our analysis we see only this localised flow. Future work might shed some light on these opened questions.

ACKNOWLEDGEMENTS

We acknowledge the work of all the people that contribute to and maintain the GPR and SOON/USAF/NOAA Sunspot databases. We also thank the anonymous referee for helping to significantly improve the quality of this paper. The research was partly funded from the European Commission's Seventh Framework Programme (FP7/2007-2013) under the grant agreements n°284461 [eHEROES] and n°312495 [SOLARNET].

REFERENCES

Arévalo M. J., Gomez R., Vázquez M., Balthasar H., Wöhl H., 1982, A&A, 111, 266
Arévalo M. J., Gomez R., Vázquez M., Balthasar H., Wöhl H., 1983, A&A, 117, 170
Balthasar H., Vázquez M., Wöhl H., 1986, A&A, 155, 87
Balthasar H., Wöhl H., 1980, A&A, 92, 111
Balthasar H., Wöhl H., 1981, A&A, 98, 422
Balthasar H., Wöhl H., Stark D., 1987, A&A, 174, 359
Basu S., Antia H. M., 2003, ApJ, 585, 553
Belvedere G., Godoli G., Motta S., Paternò L., Zappalà R. A., 1976, Sol. Phys., 46, 23
Brajša R., Ruždjak D., Wöhl H., 2006, Sol. Phys., 237, 365
Brajša R., Wöhl H., Ruždjak D., Schawinski-Guiton K., 2004, Hvar Observatory Bulletin, 28, 55
Brajša R., Wöhl H., Ruždjak D., Vršnak B., Verbanac G., Svalgaard L., Hochedez J.-F., 2007, Astronomische Nachrichten, 328, 1013
Brajša R., Wöhl H., Vršnak B., Ruždjak D., Sudar D., Roša D., Hržina D., 2002, Sol. Phys., 206, 229
Brajša R., Wöhl H., 2000, Hvar Observatory Bulletin, 24, 125
Brajša R., Wöhl H., Hanslmeier A., Verbanac G., Ruždjak D., Cliver E., Svalgaard L., Roth M., 2009, A&A, 496, 855
Canuto V. M., Minotti F. O., Schilling O., 1994, ApJ, 425, 303
Chan K. L., 2001, ApJ, 548, 1102
Duvall Jr. T. L., 1979, Sol. Phys., 63, 3
Erwin E. H., Coffey H. E., Denig W. F., Willis D. M., Henwood R., Wild M. N., 2013, Sol. Phys., 288, 157
Gilman P. A., Howard R., 1984, Sol. Phys., 93, 171
González Hernández I., Howe R., Komm R., Hill F., 2010, ApJ, 713, L16
González Hernández I., Kholikov S., Hill F., Howe R., Komm R., 2008, Sol. Phys., 252, 235
Guinan E. F., Engle S. G., 2009, in Mamajek E. E., Soderblom D. R., Wyse R. F. G., eds, IAU Symposium Vol. 258 of IAU Symposium, The Sun in time: age, rotation, and magnetic activity of the Sun and solar-type stars and effects on hosted planets. pp 395–408
Haber D. A., Hindman B. W., Toomre J., Bogart R. S., Larsen R. M., Hill F., 2002, ApJ, 570, 855
Hathaway D. H., 1996, ApJ, 460, 1027
Hathaway D. H., 2012, ApJ, 760, 84
Howard R., 1979, ApJ, 228, L45
Howard R., 1984, ARA&A, 22, 131
Howard R., Gilman P. A., 1986, ApJ, 307, 389
Howard R., Labonte B. J., 1980, ApJ, 239, L33
Howard R. F., 1991a, Sol. Phys., 136, 251
Howard R. F., 1991b, Sol. Phys., 135, 327
Howard R. F., 1996, ARA&A, 34, 75
Howe R., Christensen-Dalsgaard J., Hill F., Komm R. W., Larsen R. M., Schou J., Thompson M. J., Toomre J., 2000, ApJ, 533, L163
Hupfer C., Käpylä P. J., Stix M., 2006, A&A, 459, 935
Kambry M. A., Nishikawa J., Sakurai T., Ichimoto K., Hiei E., 1991, Sol. Phys., 132, 41
Käpylä P. J., Korpi M. J., Tuominen I., 2004, A&A, 422, 793
Komm R. W., Howard R. F., Harvey J. W., 1993, Sol. Phys., 147, 207

Lustig G., Wöhl H., 1990, A&A, 229, 224
Olemskoy S. V., Kitchatinov L. L., 2005, Astronomy Letters, 31, 706
Pérez Garde M., Vázquez M., Schwan H., Wöhl H., 1981, A&A, 93, 67
Pulkkinen P., Tuominen I., 1998, A&A, 332, 755
Pulkkinen P., Tuominen I., Brandenburg A., Nordlund Å., Stein R. F., 1993, A&A, 267, 265
Roša D., Brajša R., Vršnak B., Wöhl H., 1995, Sol. Phys., 159, 393
Rüdiger G., Hollerbach R., 2004, The magnetic universe: Geophysical and Astrophysical Dynamo Theory. Wiley-VCH, Weinheim
Ruždjak D., Brajša R., Sudar D., Wöhl H., 2005, Sol. Phys., 229, 35
Ruždjak D., Ruždjak V., Brajša R., Wöhl H., 2004, Sol. Phys., 221, 225
Schröter E. H., 1985, Sol. Phys., 100, 141
Schröter E. H., Wöhl H., 1976, Sol. Phys., 49, 19
Snodgrass H. B., Dailey S. B., 1996, Sol. Phys., 163, 21
Stix M., 1989, The Sun. an Introduction. Springer-Verlag, Berlin Heidelberg New York
Ulrich R. K., Boyden J. E., Webster L., Padilla S. P., Snodgrass H. B., 1988, Sol. Phys., 117, 291
Vršnak B., Brajša R., Wöhl H., Ruždjak V., Clette F., Hochedez J.-F., 2003, A&A, 404, 1117
Ward F., 1965, ApJ, 141, 534
Willis D. M., Coffey H. E., Henwood R., Erwin E. H., Hoyt D. V., Wild M. N., Denig W. F., 2013a, Sol. Phys., 288, 117
Willis D. M., Henwood R., Wild M. N., Coffey H. E., Denig W. F., Erwin E. H., Hoyt D. V., 2013b, Sol. Phys., 288, 141
Wöhl H., Brajša R., 2001, Sol. Phys., 198, 57
Zhao J., Kosovichev A. G., 2004, ApJ, 603, 776